Time dependent changes in Schottky barrier mapping of the W/Si(001) interface utilizing ballistic electron emission microscopy

Chris A. Durcan,[1] Robert Balsano,[1] and Vincent P. LaBella[2,a)]
[1]College of Nanoscale Science and Engineering, State University of New York, Albany, New York 12203, USA
[2]Colleges of Nanoscale Science and Engineering, SUNY Polytechnic Institute, Albany, New York 12203, USA

(Received 20 March 2015; accepted 13 June 2015; published online 24 June 2015)

The W/Si(001) Schottky barrier height is mapped to nanoscale dimensions using ballistic electron emission microscopy (BEEM) over a period of 21 days to observe changes in the interface electrostatics. Initially, the average spectrum is fit to a Schottky barrier height of 0.71 eV, and the map is uniform with 98% of the spectra able to be fit. After 21 days, the average spectrum is fit to a Schottky barrier height of 0.62 eV, and the spatial map changes dramatically with only 27% of the spectra able to be fit. Transmission electron microscopy shows the formation of an ultra-thin tungsten silicide at the interface, which increases in thickness over the 21 days. This increase is attributed to an increase in electron scattering and the changes are observed in the BEEM measurements. Interestingly, little to no change is observed in the I-V measurements throughout the 21 day period.
 [http://dx.doi.org/10.1063/1.4922972]

I. INTRODUCTION

Schottky diodes are an active area of research due to their low capacitance, recovery times, and importance in silicon based MOSFET's as source-drain contacts.[1–5] A Schottky barrier is formed at the interface between a metal and semiconductor. The chemical potential difference between the two materials causes a transfer of carriers creating an electrostatic energy barrier called the Schottky barrier.[6,7] The height of the Schottky barrier can fluctuate laterally across the interface due to chemical and physical variations at the metal-semiconductor interface.[8] To capture the nanoscale fluctuations in Schottky barrier height, Tung introduced a chemical bonding model, which predicts that the varying bonding angles between metal and semiconductor will produce a Gaussian like spread in barrier heights.[9] The Schottky-Mott model predicts the Schottky barrier height, which is the difference between the Fermi level of the metal and the electron affinity of the semiconductor. Typically, this is not observed experimentally due to effects such as metal induced gap states, defects, and semiconductor surface states.[10–15]

An ideal technique to study Schottky barriers at the nanoscale is ballistic electron emission microscopy (BEEM). In BEEM, a scanning tunneling microscopy (STM) tip is used to inject hot electrons into the metal layer of a Schottky diode while the current transmitted into the semiconductor is recorded. If injected, electrons travel through the metal film without scattering; and if the electrons carry enough perpendicular momentum to overcome the Schottky barrier, the electrons are collected as BEEM current. BEEM probes the electrostatics of the buried metal-semiconductor interface by varying the injected carrier energy and tip location with meV energy resolution (~0.02 eV) and nanometer spatial resolution, respectively.[16] This technique has been used to measure the Schottky barrier height of many different metal/semiconductor interfaces.[17–34] Im *et al*. took ~800 spectra of the Pd/SiC diode and showed a Gaussian distribution of Schottky barrier heights consistent with the Tung model.[35] For the W/n-Si(001) interface, immediately upon metal deposition, a Schottky barrier of 0.71 eV was measured. A histogram of Schottky barrier heights from 7225 spectra follows a Gaussian like distribution. The spatial maps displayed a few areas of no measured barrier height due to defects or contaminates at the interface.[36]

In this article, the W/n-Si(001) Schottky junction is repeatedly mapped to nanoscale dimensions over 21 days, where every 7 days two point *in situ* I-V (IV) measurements and BEEM Schottky barrier maps were acquired. Over the 21 day period, the percentage of spectra able to be fit decreased from 98% to 27%. Transmission electron microscopy energy dispersive x-ray spectroscopy (TEM-EDX) shows that a tungsten silicide forms upon deposition. The interface, after 21 days, appears thicker and changes its composition. We attributed the changes observed in the BEEM data to the changes to the interface over time. Interestingly, two point IV measurements show little change over the 21 day period.

II. EXPERIMENTAL

The diode fabrication was performed under high-vacuum conditions on lightly doped *n*-Si(001) substrates with resistivity of 100 Ω cm. The native silicon oxide layer was removed utilizing a standard chemical hydrofluoric acid treatment immediately prior to loading into a high vacuum (10^{-8} mbar) deposition chamber.[24,29] The tungsten was deposited onto the substrate using electron beam evaporation; the substrate was partially covered using a shadow mask creating diodes 1 mm × 2 mm. The tungsten thickness for the sample was 5 nm. A 10 nm gold layer was deposited on top of the tungsten layer to inhibit tungsten surface oxidation. The silicon substrate was unintentionally heated above room temperature due to radiative heating from the deposition source. The deposition thickness was calibrated using Rutherford backscattering spectrometry (RBS) and TEM-

a)Electronic mail: vlabella@albany.edu

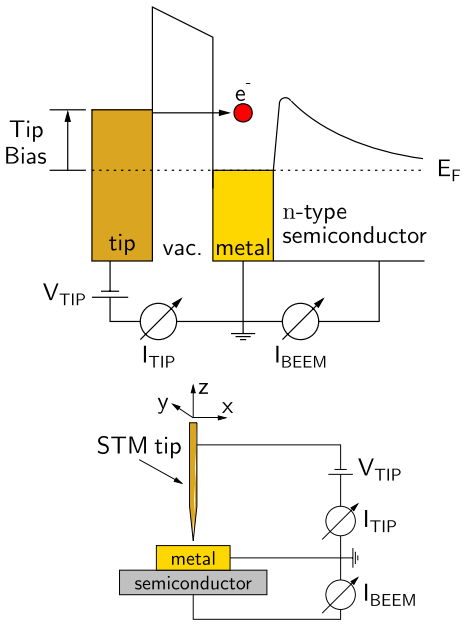

FIG. 1. (Top) Energy diagram of the BEEM setup with STM tip, metal, and n-type semiconductor. (Bottom) Wiring schematic of the BEEM setup.

EDX in a JEOL Titan. After deposition, the sample was mounted onto a custom designed sample holder for BEEM measurements. The plate allows for simultaneous grounding of both the metal film and the silicon substrate to an *ex situ* pico-ammeter to measure BEEM current. An ohmic contact was established by cold pressing indium onto the backside of the silicon substrate.

A modified low temperature STM (Omicron) was utilized for all BEEM measurements operating at a pressure in the 10^{-11} mbar range.[37] The sample was inserted into the UHV chamber within 3 h of metal deposition and loaded onto the STM stage and cooled to 80 K for all measurements. Two-point IV measurements were taken *in situ* for each sample at low temperatures using a Keithley 2400 source measurement unit to record IV characteristics. All measurements were taken in the absence of ambient light. Pt/Ir STM tips, mechanically cut at a steep angle, were utilized for all BEEM measurements. The experimental schematic and energy band diagram are shown in Fig. 1. All BEEM measurements were taken using a constant tunneling current setpoint of 20 nA with forward tip biasing, i.e., the carriers injected into the metal are electrons, the same as the majority carriers in the silicon substrate.

To obtain a BEEM spectrum, the STM tip stays at one location, while the voltage between the tip and metal surface is increased from 0.2 V to 2.0 V while recording the BEEM current. The STM tip moves to a new location and the measurement is repeated. For each series of BEEM measurements, spectra were taken every 11.7 nm throughout a $1\,\mu m \times 1\,\mu m$ area. After the initial set of spectra was taken, the sample was allowed to return to room temperature and sit under ultra high vacuum (UHV) conditions for 7 days. The sample was again cooled to 80 K, and another series of spectra was taken. This process was repeated two more times resulting in four sets of spectra, immediately after metal deposition, 7 days after deposition, 14 days after deposition, and 21 days after deposition. All of the spectra recorded were fit to the simplified form of the BEEM model $I_B \propto (V_t - \phi_b)^n$ to determine the Schottky barrier height, where I_B is the BEEM current, ϕ_b is the Schottky barrier, V_t is the tip bias, and n is a fitting exponent of 5/2, given by the Prietsch

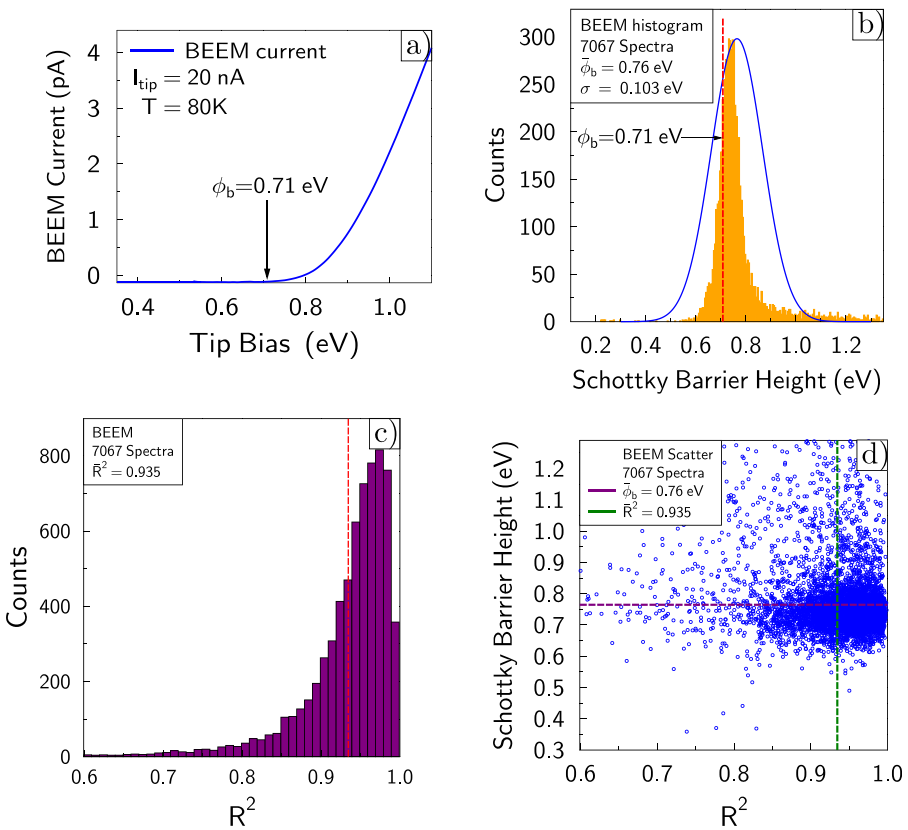

FIG. 2. (a) BEEM spectrum for initial set of spectra taken immediately after metal deposition. (b) Histogram of the 7225 Schottky barriers with a mean barrier height of 0.76 eV and dotted red line indicating the 0.71 eV Schottky barrier from the fit to the average spectrum. The Histogram has a standard deviation of 103 meV. (c) Histogram of the R^2 values with an average R^2 of 0.935. (d) R^2 vs Schottky barrier height plot for the same 7225 spectra shown in (b) with an average R^2 value of 0.935.

Ludeke (PL) fitting model.[38] The fits were preformed by linearizing the spectra and using standard linear regression, which returned the Schottky barrier and corresponding R^2 value, indicating the quality of the fit. If the fitting model cannot fit the spectrum to an R^2 value above 0.6, the spectrum is considered unable to be fit.

III. RESULTS

The average spectrum from the initial BEEM map along with the Schottky barrier height obtained from the fit is

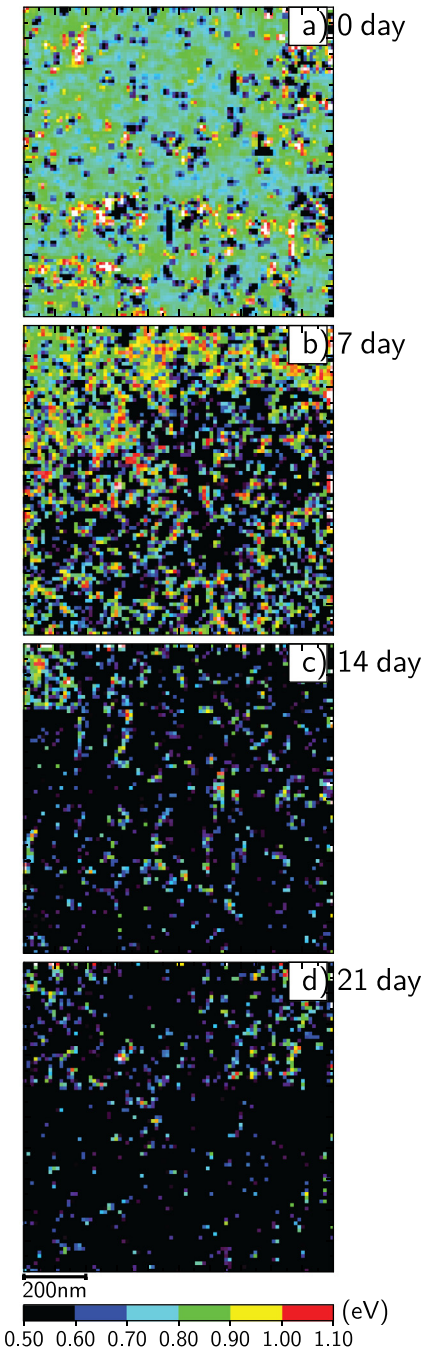

FIG. 3. (a) Schottky barrier map of the W/n-Si(001) diode immediately upon metal deposition. (b) Schottky barrier map after 7 days at room temperature and UHV conditions. (c) Schottky barrier map after fourteen days at room temperature and UHV conditions. (d) Schottky barrier map after twenty-one days at room temperature and UHV conditions.

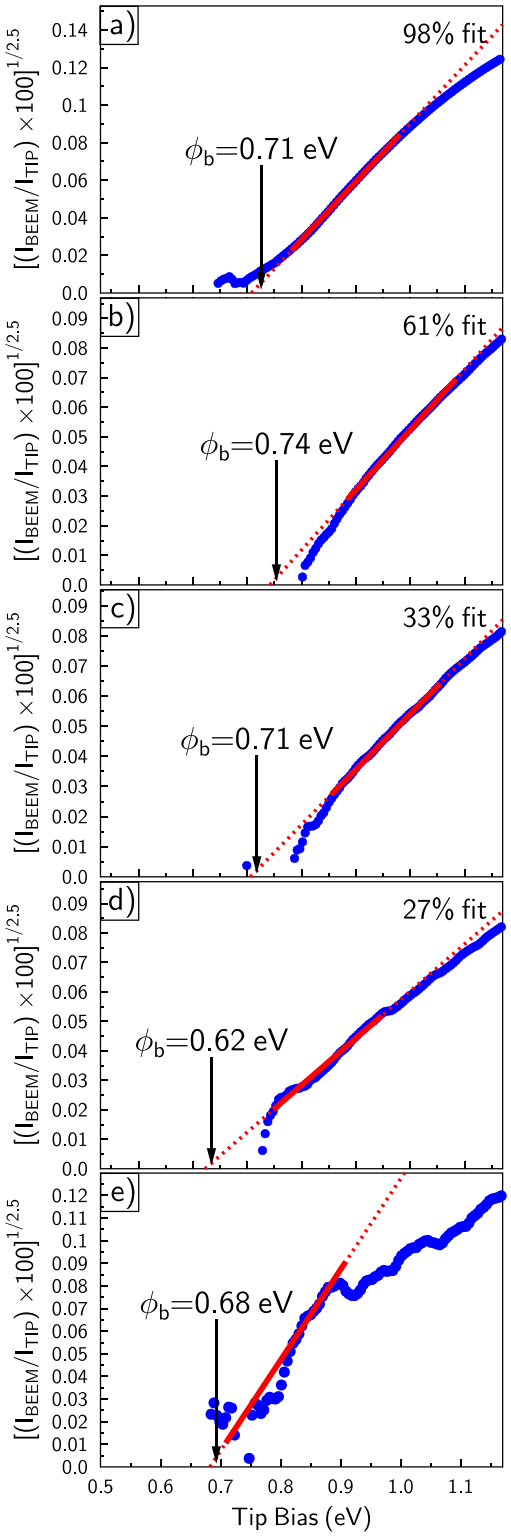

FIG. 4. (a) Average spectrum from the initial set of BEEM spectra with a Schottky barrier height of 0.71 eV, 0.005% BEEM transmission at 1.15 V bias, and 98% of the spectra able to be fit. (b) Average spectrum from the +7 day set of BEEM spectra with a Schottky barrier height of 0.74 eV, 0.002% BEEM transmission at 1.15 V bias, and 61% of the spectra able to be fit. (c) Average spectrum from the +14 day set of BEEM spectra with a Schottky barrier height of 0.71 eV, 0.002% BEEM transmission at 1.15 V bias, and 33% of the spectra able to be fit. (d) Average spectrum from the +21 day set of BEEM spectra with a Schottky barrier height of 0.62 eV, 0.002% BEEM transmission at 1.15 V bias, and 27% of the spectra able to be fit. (e) Average spectrum from (d) containing only spectra with an R^2 value greater than 0.95 with a Schottky barrier height of 0.68 eV and 0.005% BEEM transmission at 1.15 V bias.

displayed in Fig. 2(a). A histogram of all the Schottky barrier heights from each individual spectrum along with a line indicating the fit to the average spectrum is displayed in Fig. 2(b). A Gaussian distribution is drawn from the mean of the distribution, $\bar{\phi} = 0.76\,\text{eV}$, and its standard deviation, $\sigma = 103\,\text{meV}$. The Schottky barrier height distribution has a tail to higher energies (>0.9 eV). A histogram of the R^2 values is displayed in Fig. 2(c) with 78% of the spectra with $R^2 > 0.9$ and a mean R^2 value of 0.93. A scatter plot of the Schottky barrier heights vs the R^2 value is shown in Fig. 2(d). The plot shows that high R^2 values are obtained for the full range of Schottky barrier heights while also being centered around the mean Schottky barrier.

The Schottky barrier map acquired immediately after metal deposition, 7 days, 14 days, and 21 days, is shown in Figs. 3(a)–3(d), respectively. Immediately after deposition, the Schottky barrier map is uniform with 98% of the spectra fit and centered around the average Schottky barrier height of 0.76 eV. The few black spots are spectra with no fit. After 7 days, the Schottky barrier map is no longer uniform, with 61% of the spectra fit, $\bar{\phi} = 0.94\,\text{eV}$, and $\sigma = 155\,\text{meV}$. After 14 days, the Schottky barrier map consists of 33% of the spectra which could be fit, $\bar{\phi} = 0.89\,\text{eV}$, and $\sigma = 202\,\text{meV}$. After 21 days, the Schottky barrier map contains only 27% of spectra, which are able to be fit, $\bar{\phi} = 0.88\,\text{eV}$ and $\sigma = 221\,\text{meV}$.

The set of spectra for each Schottky barrier map were average together to form one representative spectrum and are shown linearized with their corresponding fit in Figs. 4(a)–4(d). The average spectra taken immediately after deposition is fit to a Schottky barrier height of 0.71 eV, an R^2 value >0.999 and 0.005% BEEM transmission at 1.15 V. The 7 day sample is fit to a Schottky barrier of 0.74 eV, an R^2 value of 0.997, and 0.002% BEEM transmission at 1.15 V. The 14 day sample is fit to a Schottky barrier of 0.71 eV, an R^2 value of 0.997, and 0.002% BEEM transmission at 1.15 V. The 21 day sample is fit to a Schottky barrier of 0.62 eV, an R^2 value of 0.98 and 0.002% BEEM transmission at 1.15 V. Fig. 4(e) is the average of all the spectra from Fig. 4(d) that have a fit with an $R^2 > 0.95$ and is fit to a Schottky barrier of 0.68 eV with 0.005% BEEM transmission at 1.15 V.

The results of the TEM and EDX measurements for the interface immediately after deposition are shown in Figs. 5(a) and 5(b). The mass percentages of tungsten, gold, silicon, and oxygen are plotted in Fig. 5(a) with an image across the interface shown in Fig. 5(b). The EDX and TEM measurements of the diode in Figs. 5(a) and 5(b) are taken within 24 hours of metal deposition. The percentage of gold at the tungsten to silicon interface is negligible as well as the percentage of oxygen. The intermixed region is ~1.4 nm thick and composed entirely of silicon and tungsten. The EDX and TEM measurements of the diode 21 days after the metal deposition are shown in Figs. 5(c) and 5(d). The mass percentages of tungsten, gold, silicon, and oxygen are plotted in Fig. 5(c) with an image across the interface shown in Fig. 5(d). The intermixed region has increased its thickness to ~3.8 nm while the percentage of gold is still negligible. There also appears to be a small oxygen concentration at the interface.

Two point IV curves acquired *in situ* are displayed in Figs. 6(a)–6(d). The IV curves show little deviation from each other with a linear fit to the forward bias current showing only small changes to the slope or intercept. All of the IV curves are taken immediately before BEEM measurements.

IV. DISCUSSION

The Schottky barrier height of the average spectra is approximately 50 meV lower than the mean of the distribution, arising from the broad distribution of Schottky barrier heights obtained from fitting the thousands of individual spectra. Averaging a collection of spectra with a distribution of onset biases results in an average spectrum favoring a lower onset, which is picked out by the fitting routine. The distribution of onset voltages also explains the ~70 meV

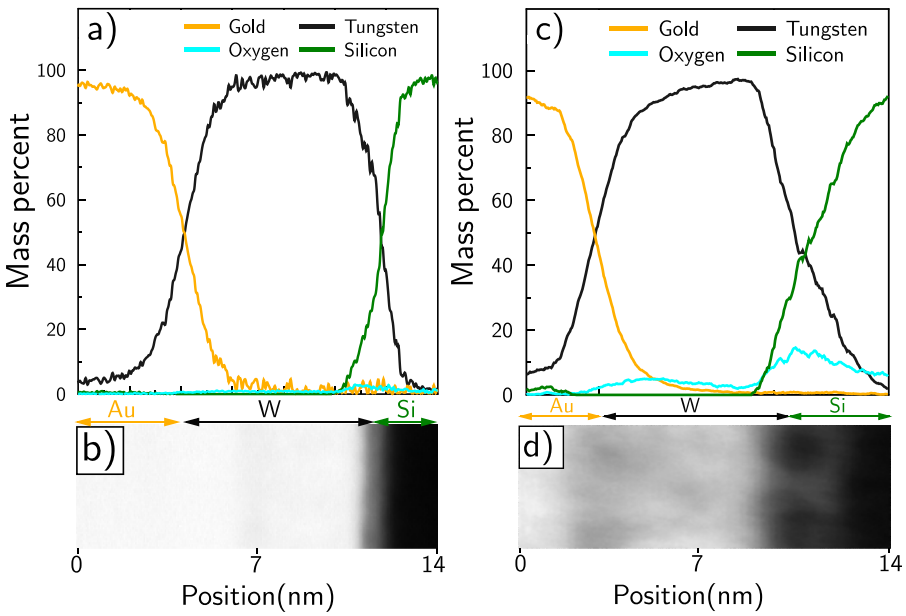

FIG. 5. (a) EDX line scan of the W/n-Si(001) Schottky diode immediately after metal deposition, showing atomic percentages of Au, W, O, and Si. (b) TEM image of EDX scan in (a). (c) EDX line scan of the W/n- Si(001) Schottky diode 21 days after metal deposition, also showing atomic percentages of Au, W, O, and Si. (d) TEM image of the EDX scan in (c).

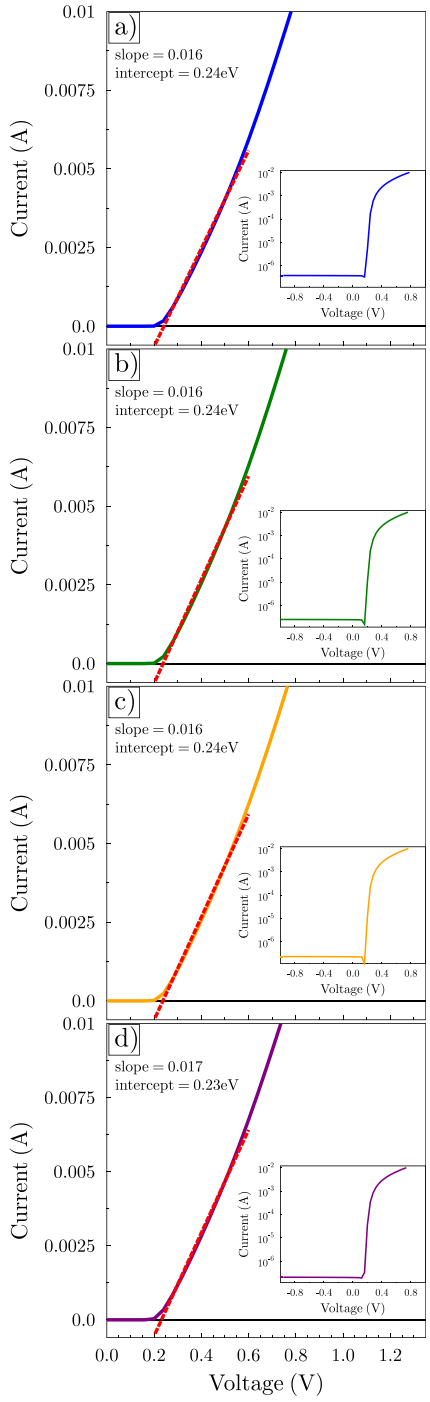

FIG. 6. (a) Two point I-V curve for the W/n-Si(001) diode immediately after metal deposition with linear fit to forward bias region. Inset is the full diode rectification with reverse bias current $\sim 10^{-7}$ A. Measurement taken at 80 K without ambient light. (b) Two point I-V curve taken on the +7 day sample showing little change in forward bias current compared to (a). Inset is the full diode rectification with reverse bias current $\sim 10^{-7}$ A. (c) Two point I-V curve taken on the +14 day sample showing little change in rectifying current. Inset is the full diode rectification with reverse bias current $\sim 10^{-7}$ A. (d) Two point I-V curve taken on the +21 day sample again showing little change in rectifying current. Inset is the full diode rectification with reverse bias current $\sim 10^{-7}$ A.

difference between the Schottky barrier height and the start of the fit (solid red line) that is observed in the linearized spectra shown in Fig. 4(a). The averaged spectrum and Schottky barrier obtained from the fit clearly do not capture the complicated nature of the electrostatics that is present at the interface. The broad distribution of barrier heights is indicative of an electrostatically varying interface arising from the structural disorder due to the intermixed tungsten and silicon.

Although the majority of spectra fit to a Gaussian distribution centered around the mean Schottky barrier height (0.76 eV), there are locations at the interface with higher barrier heights ($\phi_b > 0.9$ eV), several standard deviations above the mean. The R^2 value of these higher barrier heights are of high quality, >0.9, as displayed in Fig. 2(d). These higher barrier heights form small localized clusters (2–10 tip locations) that are distributed randomly over the interface as seen in Fig. 3(a). A locally higher barrier height can arise due to a change in the interface, such as a defect, or the presence of a foreign material at the interface such as an oxide cluster. In addition, a physical defect that increases the elastic scattering can also give rise to a locally higher barrier due to the narrow acceptance cone of parallel momentum states just above the barrier.

A dramatic change is observed in measured electrostatics of the interface when the BEEM measurements are taken over the course of 21 days. The marked decrease in the percentage of spectra that can be fit to a Schottky barrier height indicates that structure of the interface is changing. The decrease in the Schottky barrier height for the 21 day sample is caused by averaging numerous spectra with little or no signal increasing the noise and making it difficult for the fitting routine to obtain a good fit as evidenced in the lower R^2 value. To reduce the amount of noise in the spectra for the 21 day sample, an average spectrum was created only from the spectra that had fits with an R^2 value above 0.95, which resulted in a higher barrier height of 0.68 eV and an increase in transmission current, closer to the as-deposited sample. This selective averaging method can be utilized as a powerful noise reduction method for future BEEM studies and may be useful for future BEEM studies, where there is a low amount of transmission current.

The formation of the interfacial silicide was not accelerated by sample annealing as the sample was left at room temperature under UHV conditions over the 21 day period of study. Upon metal deposition, the interface is comprised of tungsten and silicon, with a 1.4 nm region of uniformly intermixed tungsten and silicon as seen in the TEM results displayed in Fig. 5(b). This initial intermixing is accelerated due to the unintentional heating during the deposition process. After 21 days, the interface appears dramatically different, with a much less uniform intermixed region of tungsten and silicon that is approximately 3.8 nm thick. The small oxygen peak at the interface is attributed to the TEM sample fabrication process. The +21 day TEM sample spent additional time exposed to atmosphere between fabrication and TEM imaging, as compared to the TEM sample immediately following metal deposition. This increase in oxygen concentration only affected the TEM measurement as the BEEM sample was kept under UHV conditions. The TEM measurements did not detect gold at the interface for either sample. The observed changes to the tungsten silicon interface attributed to the dramatic change in the BEEM data, characterized by the 118 meV increase in standard deviation of Schottky

distributions and drastic reduction in spectra able to be fit over the 21 days. The attenuation of the ballistic electrons increases as the intermixed region increases in both thickness and disorder. This will result in numerous spectra with little or no current and hence, no detectible Schottky barrier. Small changes to the interface in disorder or thickness can induce drastic changes to the BEEM spectra. This is shown in the decrease in BEEM current from 0.005% in the initial average BEEM spectra to 0.002% in the 21 day average BEEM spectra. After 21 days, the interface becomes thicker and more disordered. When an average spectrum is created from the individual BEEM spectra with a fit to $R^2 > 0.95$, the BEEM current returned to 0.005%. This indicates that there are local areas of the interface that allow similar amounts of transmission as when the interface was just formed.

Interestingly, the two point I-V curves displayed in Fig. 6 show little to no variation in reversed bias current, forward bias slope, or intercept even with the observed changes to the interface seen in TEM and BEEM measurements. This demonstrates the utility of the BEEM technique to map changes in the electrostatics of a buried interface to nanoscale dimensions that go unnoticed with conventional macroscopic spectroscopy methods.

V. CONCLUSION

Utilizing BEEM, the changes in the W/Si(001) interface over time were measured and show changes to the transmission of ballistic electrons as the interface evolves. The initial set of BEEM spectra show an interface visible to ballistic electrons with a Schottky barrier of 0.71 eV. Over the course of 21 days, the interface changes in structure causing the interface the completely scatter ballistic electrons and inhibit the ability to accurately measure a Schottky barrier. TEM measurements show the interfacial silicide, which forms upon deposition grows in thickness over time at room temperature. I-V measurements taken alongside BEEM data show no change to the electronic structure of the W/Si diode. These results demonstrate BEEM's sensitivity to changes in the interface electrostatics with nanoscale resolution that is not possible with the conventional IV spectroscopy.

ACKNOWLEDGMENTS

The authors acknowledge the support of the Semiconductor Research Corporation, Center for advanced Interconnect Science and Technology, the National Science Foundation Grant DMR-1308102, and SEMATECH.

[1]B. E. Coss, P. Sivasubramani, B. Brennan, P. Majhi, R. M. Wallace, and J. Kim, J. Vac. Sci. Technol., B **31**, 021202 (2013).
[2]S. Smith, K. Aouadi, J. Collins, E. van der Vegt, M.-T. Basso, M. Juhel, and S. Pokrant, Microelectron. J. **82**, 261 (2005).
[3]S. Haimsona, Y. Shacham-Diamand, D. Horvitz, and A. Rozenblat, Microelectron. Eng. **92**, 134 (2012).
[4]F. Papadatos, K. Wong, V. Arunachalam, C. H. Shin, Z. Li, M. Chudzik, W.-H. Lee, and A. Xing, Microelectron. Eng. **92**, 123 (2012).
[5]M. Tsai, H. Chao, L. Ephrath, B. Crowder, A. Cramer, R. Bennett, C. Lucchese, and M. Wordeman, J. Electrochem. Soc. **128**, 2207 (1981).
[6]S. K. Cheung and N. W. Cheung, Appl. Phys. Lett. **49**, 85 (1986).
[7]T. Arizumi and M. Hirose, Jpn. J. Appl. Phys. **8**, 749 (1969).
[8]R. T. Tung, Appl. Phys. Lett. **58**, 2821 (1991).
[9]R. T. Tung, Phys. Rev. Lett. **84**, 6078 (2000).
[10]R. T. Tung, Phys. Rev. B **45**, 13509 (1992).
[11]R. Tung, Applied Phys. Rev. **1**, 011304 (2014).
[12]H. Palm, M. Arbes, and M. Schulz, Phys. Rev. Lett. **71**, 2224 (1993).
[13]A. E. Fowell, R. H. Williams, B. E. Richardson, A. A. Cafolla, D. I. Westwood, and D. A. Woolf, J. Vac. Sci. Technol., B **9**, 581 (1991).
[14]A. E. Fowell, R. H. Williams, B. E. Richardson, and T. H. Shen, Semicond. Sci. Technol. **5**, 348 (1990).
[15]A. Olbrich, J. Vancea, F. Kreupl, and H. Hoffmann, J. Appl. Phys. **83**, 358 (1998).
[16]M. Prietsch, Phys. Rep. **253**, 163 (1995).
[17]M. K. Weilmeier, W. H. Rippard, and R. A. Buhrman, Phys. Rev. B **59**, R2521 (1999).
[18]M. K. Weilmeier, W. H. Rippard, and R. A. Buhrman, Phys. Rev. B **61**, 7161 (2000).
[19]W. J. Kaiser, M. H. Hecht, R. W. Fathauer, L. D. Bell, E. Y. Lee, and L. C. Davis, Phys. Rev. B **44**, 6546 (1991).
[20]H. Sirringhaus, T. Meyer, E. Y. Lee, and H. von Känel, Phys. Rev. B **53**, 15944 (1996).
[21]C. A. Bobisch, A. Bannani, Y. M. Koroteev, G. Bihlmayer, E. V. Chulkov, and R. Moller, Phys. Rev. Lett. **102**, 136807 (2009).
[22]C. A. Ventrice, Jr., V. P. LaBella, G. Ramaswamy, H. P. Yu, and L. J. Schowalter, Phys. Rev. B **53**, 3952 (1996).
[23]I. Sitnitsky, J. J. Garramone, J. Abel, P. Xu, S. D. Barber, M. L. Ackerman, J. K. Schoelz, P. M. Thibado, and V. P. LaBella, J. Vac. Sci. Technol., B **30**, 04E110 (2012).
[24]J. J. Garramone, J. R. Abel, I. L. Sitnitsky, L. Zhao, I. Appelbaum, and V. P. LaBella, Appl. Phys. Lett. **96**, 062105 (2010).
[25]H. J. Im, B. Kaczer, J. P. Pelz, and W. J. Choyke, Appl. Phys. Lett. **72**, 839 (1998).
[26]C. Tivarus, J. P. Pelz, M. K. Hudait, and S. A. Ringel, Phys. Rev. Lett. **94**, 206803 (2005).
[27]T. Banerjee, E. Haq, M. Siekman, J. Lodder, and R. Jansen, IEEE Trans. Magn. **41**, 2642 (2005).
[28]J. J. Garramone, J. R. Abel, S. Barraza-Lopez, and V. P. LaBella, Appl. Phys. Lett. **100**, 252102 (2012).
[29]J. J. Garramone, J. R. Abel, I. L. Sitnitsky, and V. P. LaBella, J. Vac. Sci. Technol., A **28**, 643 (2010).
[30]J. J. Garramone, J. R. Abel, I. L. Sitnitsky, R. L. Moore, and V. P. LaBella, J. Vac. Sci. Technol., B **27**, 2044 (2009).
[31]A. J. Stollenwerk, M. R. Krause, D. H. Idell, R. Moore, and V. P. LaBella, J. Vac. Sci. Technol., B **24**, 2009 (2006).
[32]A. Stollenwerk, M. Krause, R. Moore, and V. P. LaBella, J. Vac. Sci. Technol., A **24**, 1610 (2006).
[33]H. L. Qin, K. E. J. Goh, M. Bosman, K. L. Pey, and C. Troadec, J. Appl. Phys. **111**, 013701 (2012).
[34]S. Forment, R. L. Van Meirhaeghe, A. D. Vrieze, K. Strubbe, and W. P. Gomes, Semicond. Sci. Technol. **16**, 975 (2001).
[35]H. J. Im, Y. Ding, J. P. Pelz, and W. J. Choyke, Phys. Rev. B **64**, 075310 (2001).
[36]C. A. Durcan, R. Balsano, and V. P. LaBella, J. Appl. Phys. **116**, 023705 (2014).
[37]M. Krause, A. Stollenwerk, C. Awo-Affouda, B. Maclean, and V. P. LaBella, J. Vac. Sci. Technol., B **23**, 1684 (2005).
[38]M. Prietsch and R. Ludeke, Phys. Rev. Lett. **66**, 2511 (1991).